Alterations of uromodulin biology: a common denominator of the genetically heterogeneous FJHN/MCKD syndrome

P Vylet'al[1,2,8], M Kublová[1,2,8], M Kalbáčová[1,2], K Hodaňová[1,2], V Barešová[1,2], B Stibůrková[2], J Sikora[2], H Hůlková[2], J Živný[3], J Majewski[4], A Simmonds[5], J-P Fryns[6], G Venkat-Raman[7], M Elleder[2] and S Kmoch[1,2]

[1]Center for Applied Genomics, Charles University 1st School of Medicine, Prague, Czech Republic; [2]Institute for Inherited Metabolic Disorders, Charles University 1st School of Medicine, Prague, Czech Republic; [3]Department of Pathophysiology, Charles University 1st School of Medicine, Prague, Czech Republic; [4]Department of Human Genetics, McGill University and Genome Quebec Innovation Center, Montreal, Quebec, Canada; [5]Purine Research Unit, GKT, Guy's Hospital, London, UK; [6]Center for Human Genetics, University of Leuven, Leuven, Belgium and [7]Renal Unit, Queen Alexandra Hospital, Portsmouth, UK

Autosomal dominant hyperuricemia, gout, renal cysts, and progressive renal insufficiency are hallmarks of a disease complex comprising familial juvenile hyperuricemic nephropathy and medullary cystic kidney diseases type 1 and type 2. In some families the disease is associated with mutations of the gene coding for uromodulin, but the link between the genetic heterogeneity and mechanism(s) leading to the common phenotype symptoms is not clear. In 19 families, we investigated relevant biochemical parameters, performed linkage analysis to known disease loci, sequenced *uromodulin* gene, expressed and characterized mutant uromodulin proteins, and performed immunohistochemical and electronoptical investigation in kidney tissues. We proved genetic heterogeneity of the disease. *Uromodulin* mutations were identified in six families. Expressed, mutant proteins showed distinct glycosylation patterns, impaired intracellular trafficking, and decreased ability to be exposed on the plasma membrane, which corresponded with the observations in the patient's kidney tissue. We found a reduction in urinary uromodulin excretion as a common feature shared by almost all of the families. This was associated with case-specific differences in the uromodulin immunohistochemical staining patterns in kidney. Our results suggest that various genetic defects interfere with uromodulin biology, which could lead to the development of the common disease phenotype. 'Uromodulin-associated kidney diseases' may be thus a more appropriate term for this syndrome.

Kidney International advance online publication, 2 August 2006; doi:10.1038/sj.ki.5001728

KEYWORDS: familial nephropathy; genetic renal disease; uromodulin; Tamm–Horsfall protein; hyperuricemia

Correspondence: *S Kmoch, Center for Applied Genomics, Institute for Inherited Metabolic Disorders, Ke Karlovu 2, 128 00 Prague 2, Czech Republic. E-mail: skmoch@lf1.cuni.cz*

[8]These authors contributed equally to this work

Received 18 January 2006; revised 7 June 2006; accepted 13 June 2006

Familial juvenile hyperuricemic nephropathy (FJHN) (OMIM 162000),[1,2] and medullary cystic kidney diseases type 1 (MCKD1; OMIM 174000),[3] and type 2 (MCKD2; OMIM 603860)[4] are autosomal dominant tubulointerstitial nephropathies characterized by combinations of hyperuricemia, gouty arthritis, progressive renal insufficiency, and in some but not all families, medullary cysts. Recently it was found that in some families FJHN and MCKD2 are allelic disorders associated with mutations of the uromodulin gene (*UMOD*) coding for uromodulin (UMOD), Tamm–Horsfall protein.[5–12] However, *UMOD* mutations are not the only cause of the FJHN/MCKD phenotype,[8,9] which confirmed the broader genetic heterogeneity suggested by linkage studies.[13–18] The other candidate loci for FJHN/MCKD were identified on chromosome 1q21,[18–21] chromosome 1q41,[22] and a disease causing mutation in *HNF-1β* gene was found in a single family with features of FJHN and diabetes.[23] The mechanism linking the genetic heterogeneity to common disease symptom development in families with no *UMOD* mutations is not clear but it was suggested that UMOD dysfunction might be a common pathogenic mechanism.[22]

In this study, we have investigated 19 families showing characteristics of the FJHN/MCKD phenotype. In all families we performed linkage analysis to all known FJHN/MCKD loci, and analyzed the *UMOD* genomic sequence. Disease causing *UMOD* mutations were identified in only six families. We transiently expressed mutant proteins in eucaryotic cells and correlated its properties with biochemical, immunohistochemical, electron microscopy observations and specific disease symptoms. We also found that decreased urinary UMOD excretion is common to almost all patients independent of their corresponding linkage groups. The changes in urinary UMOD excretion were accompanied by case-specific differences of UMOD immunohistochemical staining patterns in kidney tissues.

Our work suggests that various genetic defects and mechanisms hamper UMOD biology, which lead to the

development of the FJHN/MCKD phenotype, and this lends support to the term of 'uromodulin-associated kidney diseases' (UAKD)[5,22] as a more appropriate for the FJHN/MCKD syndrome.

RESULTS

Clinical and biochemical findings

The pedigrees of families not yet reported are shown in Figure 1.

The family CZ4 came to attention through the probands N IV.3 (39 years old), and N IV.4 (31 years old), who suffered from gout. Biochemical investigation showed hyperuricemia, reduced fractional excretion of uric acid, and elevated concentration of plasma creatinine. Urinary UMOD excretion was absent. Their father N III.3 (62 years old) suffered from gout, which appeared for the first time at 23 years of age. He gradually developed renal insufficiency, which was treated at 55 years of age by dialysis and two years later by renal transplantation.

The family CZ5 came to attention through the proband F II.1 who suffered from gout, which appeared for the first time at 26 years of age. Biochemical investigation showed hyperuricemia (over 700 μmol/l), reduced fractional excretion of uric acid (5.9%), and elevated concentration of plasma creatinine (204 μmol/l). Following treatment with allopurinol, uricemia normalized, but the gouty attacks have persisted and patient (now 36 years old) has developed hypertension and chronic renal insufficiency. Sonography showed bilateral small kidneys with reduced parenchyma and single cyst (5 mm). Urinary UMOD excretion was absent. Molecular investigation revealed a pathogenic mutation resulting in C32Y substitution in UMOD protein. All the relatives have been reported healthy, their biochemical investigations showed no abnormalities, molecular investigation has not revealed in any of them the presence of pathogenic *UMOD* mutation. The possibility of nonpaternity was excluded by STR analysis.

The family US1 came to attention through the proband US I.1., who developed gout during pregnancy at the age of 27 years. Biochemical investigation showed hyperuricemia which did not responded to any treatment, reduced fractional excretion of uric acid and elevated concentration of plasma creatinine (185 μmol/l). Sonography showed small kidneys and renal biopsy revealed glomerular sclerosis and glomerular cysts. Individuals US II.1 (23 years old) and US II.2 (21 years old) showed hyperuricemia (>700 μmol/l), elevated concentration of plasma creatinine (>200 μmol/l), and urea (>7.5 mmol/l). Both patients responded to allopurinol and had no further gout. No urine was available for investigation of UMOD excretion.

The other families have been described previously.[13,15,18,24,25] The diagnosis of FJHN/MCKD was based on the familial occurrence of chronic renal disease associated with or preceded by early onset of hyperuricemia associated with reduced fractional excretion of uric acid $<5\%$. Biochemical investigations showed no notable abnormalities in other serum ion concentration. Urine biochemical parameters measured in available individuals are shown in Table 1. Clinical information on individuals with *UMOD* mutations is provided in Table 2.

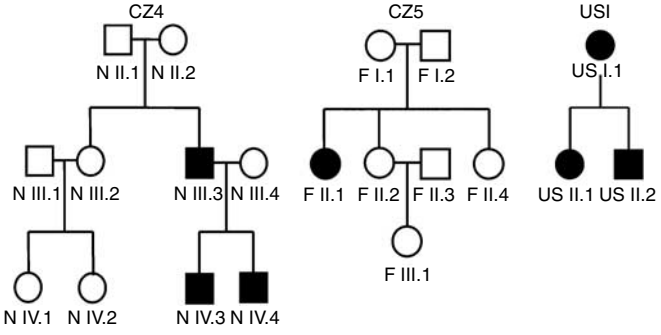

Figure 1 | Pedigree diagram of the investigated and not yet reported UAKD families. Black symbols denote affected individuals, open symbols denote unaffected individuals.

Genotyping and linkage analysis

Linkage analyses to the *UMOD* candidate locus in 16 families have been reported previously.[13,15] Families US1, CZ4, and CZ5 are reported here for the first time. As summarized in Table 3, the genetic linkage to the *UMOD* candidate locus on chromosome 16p11.2 was found in nine of the analyzed families and excluded, based on the logarithm of odds (LOD) $=-2$ criterion, in three families. A single family BE1 has been linked to UAKD locus on 1q41 previously[22] and in family GB4, a disease-causing mutation in *HNF-1β* gene was found.[23] In the rest of the families, no consistent haplotypes segregating with any of the currently known FJHN/MCKD loci were found.

UMOD gene analysis

Sequence analysis revealed missense mutations in six families (Table 3, Figure 2) and several novel single-nucleotide polymorphisms (Table 4). In families, which showed genetic linkage to the *UMOD* candidate locus on chromosome 16p11.2, and in which no *UMOD* mutation was identified, the 5.7-kb promoter sequence of the *UMOD* gene was also analyzed. Identified nucleotide changes are shown in Table 4.

Transient expression of UMOD

We cloned wild type and identified mutated *UMOD* cDNA sequences into mammalian expression vector and transiently expressed wt-UMOD protein in HEK-293, MDCK, CHO, and AtT-20 cells. The UMOD processing and localization patterns were essentially identical in all the cell lines (data not shown).[26] AtT-20 cells were chosen for further experiments as they were the most easy to culture, showed higher transfection efficiency, and performed best with available compartment markers antibodies.

Flow cytometry

The amount of the UMOD expressed on the plasma membrane was measured 6, 12, 18, and 24 h after transfection

Table 1 | Urine biochemical parameters measured in patients with mutation in *UMOD* gene (*UMOD*+), in patients with no mutation in *UMOD* gene (*UMOD*−), and in controls

Parameter	*UMOD*+ (*n*)	*P*	*UMOD*− (*n*)	*P*	Control (*n*=77)
Age	40±18 (21)	NS	40±16 (11)	NS	36±13
Creatinine (mmol/l)	6.5±3.2 (16)	NS	7.8±4.7 (31)	NS	9.0±5.4
Na/Cr (mmol/mmol)	13.9±7.9 (16)	NS	12.4±8.0 (31)	NS	13.9±8.8
K/Cr (mmol/mmol)	4.93±1.74 (16)	NS	4.45±2.18 (31)	⩽0.05	6.54±4.30
Mg^{2+}/Cr (mmol/mmol)	0.30±0.11 (14)	NS	0.29±0.18 (24)	NS	0.37±0.27
PO_4/Cr (mmol/mmol)	1.80±0.67 (14)	NS	2.01±1.27 (24)	NS	1.96±1.22
Cl/Cr (mmol/mmol)	12.3±7.5 (16)	NS	10.6±6.7 (31)	⩽0.01	17.2±11.6
Ca^{2+}/Cr (mmol/mmol)	0.19±0.19 (14)	⩽0.05	0.10±0.10 (24)	⩽0.0001	0.35±0.25
Osmolality (mOsm/kg)	329±65 (14)	⩽0.01	414±88 (13)	⩽0.05	572±278
UCB/Cr (mg/mmol)	69±167 (16)	⩽0.001	30±47 (31)	⩽0.001	8.5±8.7
UA/Cr (mmol/mol)	103±81 (14)	⩽0.0001	120±90 (24)	⩽0.0001	247±109
Umod/Cr (mg/g)	1.8±5.5 (14)	⩽0.0001	9.1±14.7 (32)	⩽0.0001	35.7±17.8

Values are reported as means±s.d.; *P*-values (*t*-test) correspond to the comparisons between the corresponding group and controls.
Cr, creatinine; NS, not significant; UA, uric acid; UCB, total protein.

Table 2 | Clinical information on individuals and families in which UMOD mutations were identified

Family (ID)	Sex/age	Age of onset	First symptoms	Blood pressure	Gout	Cr	UA	Renal ultrasound	Present status
Family CZ1, kindred A in Stiburkova et al[13]									
AI2	F/†	30y	Gout	+/?	+/30y	+/?	+/?	SK/single C	TR 58y; †63y
AII3	F/52y	18y	Gout	+/25y	+/18y	+/18y	+18y	SK, no C	RKF, arthritis
AII5	M/55y	20y	Gout	+/40y	+/20y	+/20y	+20y	SK, no C	TR 54y, no problems
AIII2	F/22y	6y[a]	HU	+/17y	No	+/6y	+/6y	SK, no C	No problems
AIII3	M/25y	12y[a]	HT	+/12y	No	+/12y	+/6y	Normal	RKF
Family CZ2, kindred B in Stiburkova et al[13]									
BI2	F/†	NA	NA	NA	NA	NA	NA	NA	RF/†49y
BI3	M/†	NA	NA	NA	+/?	NA	NA	NA	RF/†56y
BII1	M/39y	26y	Gout	NA	+/26y	+/31	+/26y	NA	RKF
BII2	M/53y	20y	Gout, HU	+/40y	+/20y	+/25y	+/20y	SK/multiple C	RKF
BII6	M/55y	17y	Gout	+/25y	+/?	+/20y	+/20y	NA	RF, TR 28y, 42y
BII9	F/53y	20y	HT	+/?	+/30y	+/23y	+/25y	SK/multiple C	RF, TR 43y
BIII1	F/31y	17y	Gout	+/23y	+/17y	+/17y	+/17y	SK/single C	RKF
BIII2	M/28y	15y[a]	FH	No	No	+/22y	+/15y	Normal	No problems
BIII3	F/27y	10y[a]	FH	+/25y	+/10y	+/10y	+/10y	Normal	No problems
BIII7	F/29y	24y[a]	FH	+/29y	No	+/26y	+/24y	Normal	HT
Family CZ5 (this report)									
II1	F/36y	26y	Gout	+/28y	+/26y	+/26y	+/26y	Normal	HT, obesity
Family BE[2], (15)									
EII3	M/68y	20y	Albuminuria	NA	+/30y	+/30y	+/30y	NA	TR 65y, no problems
EII4	M/62y	20y	Gout	NA	+/20y	+/20y	+/20y	NA	60y, hemodialysis
EII5	M/NA	40y	Gout	NA	+/40y	+/40y	+/40y	NA	NA
Family GB2[25]									
C4	F/†	31y	Gout	+/31y	+/31y	+/31y	+/31y	NA	TR; †36y
C1	F/43y	19y[a]	HU	No	No	No	No	No	No problems
C2	M/40y	16y[a]	HU	No	No	No	No	No	No problems
Family GB7, kindred 6 in McBride et al[24]									
L7	F	NA	HU	NA	+/?	NA	NA	NA	RF
L4	F	NA	HU	NA	+/?	NA	NA	NA	NA
L12	F	NA	HU	NA	NA	NA	NA	NA	NA
L10	F/†	15y	Gout	+/25y	+/15y	NA	NA	NA	Dialysis; †63y
L15	M	NA	HU	NA	NA	NA	NA	NA	NA

[a]Or when the first signs of the disease were recognized; +/y, + the symptom is present/age of onset.
C, renal cysts; Cr, serum (plasma) creatinine; FH, family history; HU, hyperuricemia; HT, hypertension; NA, not available; RF, renal failure; RKF, reduced kidney function; SK, small kidney size; TR, kidney transplantation; UA, serum (plasma) uric acid; UMOD, uromodulin; y, years.
†Died.

Table 3 | Summary of linkage analysis to all of currently known FJHN/MCKD loci with results of *UMOD* sequence analysis

Family	UMOD 16p11.2	UMOD mutation	MCKD1 1q21	UAKD 1q41
CZ1	+	C317Y	ND	ND
CZ2	+	M229R	ND	ND
CZ3	Ex	No	Ex	Ex
BE1	Ex	No	Ex	+
BE2	+	V273F	ND	ND
GB1	–	No	Ex	–
GB2	+	C126R	ND	Ex
GB3	+	No	–	–
GB4[a]	Ex	ND	ND	Ex
GB5	–	No	–	Ex
GB6	–	No	–	–
GB7	–/+[b]	P236L	ND	ND
GB8	+	No	ND	–
GB9	–	No	–	–
GB10	–	No	–	–
MCKD6	–	No	–	–
CZ4	+	No	–	–
CZ5	ND	C32Y	ND	ND
US1	+	No	–	–

Ex, families excluded for linkage on LOD $\leqslant -2$ criterion; +, Families segregating haplotypes consistent with linkage; –, Families with haplotypes inconsistent with linkage. ND, not done.
[a]Family GB4 with a disease-causing mutation in *HNF-1β* gene.
[b]Changing the original status in person L11 (GB7) to healthy, the LOD for that family goes up from –0.49 (before) to 1.47 (now) and the haplotypes are consistent with linkage.
FJHN, familial juvenile hyperuricemic nephropathy; LOD, Logarithm of odds; MCKD, medullary cystic kidney diseases; ND, not done; UMOD, uromodulin.

(Figure 3a). The time-course experiments showed a gradual increase of the wild-type UMOD protein expressed on plasma membrane with a plateau being reached in 18–24 h. Mutant proteins – 32Y, 229R, and 317Y (group I mutants) – showed patterns similar to the wild-type protein but the amount of protein localized on the plasma membrane was always lower as compared to the wild-type protein. The other mutant proteins – 126R, 236L, and 273F (group II mutants) showed a poor ability to reach the plasma membrane as compared to both, wild-type protein and group I mutants. The differences were statistically significant when measured 18 h post-transfection (Figure 3b).

SDS-PAGE and Western blot analysis

UMOD protein was analyzed in cell lyzates and medium (Figure 4). Wild-type protein was present in two 85 and 71 kDa zones (Figure 4a) as observed previously.[26] Both zones were smeared as they were probably composed of several poorly resolved bands corresponding to heterogeneous oligosaccharide processing of UMOD.[27] Complex deglycosylation treatment with peptide *N*-glycosidase F (PNGase F, Figure 4c), sialidase A (Figure 4e), and endo-*O*-glycosidase (Figure 4b) showed that both zones represent different UMOD glycoforms. The 85 kDa zone represents properly glycosylated, glycosyl-phosphatidylinositol (GPI)-modified and membrane-anchored UMOD protein as it corresponds to that of the molecular weight of UMOD excreted in urine. The 71 kDa zone represents a UMOD precursor probably lacking branched sialic acids and terminal sialic acid residues as its molecular weight corresponds to that of the 71 kDa zone appearing after the treatment of the urinary and recombinant wt-UMOD with sialidase A (Figure 4e). This 71 kDa UMOD precursor probably accumulates owing to protein overexpression, as it is not markedly observed in a stable UMOD-expressing cell line (Figure 4f), and probably represents a protein intermediate along the secretory pathway. No detectable effect on the wild-type mobility was observed after endo-*O*-glycosidase treatment (Figure 4b), which suggests that either no significant *O*-glycosylation of UMOD occurs in AtT-20 cells, or that the action of the enzyme is blocked by extended modification of the core structure by other saccharides.[28] In agreement with Rindler *et al.*,[26] neither wild-type and later nor any of the mutant UMOD proteins were detected in medium of cultured cells (data not shown).

As seen in Figure 4a, group I mutants – 32Y, 229R, and 317Y – showed similar amounts of the fully processed 85 kDa form as the wild-type protein. The 229R mutant differed from the other two by the absence of 71 kDa form and the appearance of a 69 kDa band, which probably corresponds to the endoplasmic reticulum (ER)-retained intermediate lacking GPI anchor (see below) and missing Golgi-mediated glycosylation trimming. Group II mutants showed low amounts of the fully processed 85 kDa form and retention of the 69 kDa intermediate protein.

Following the treatment of expressed proteins with PNGase F (Figure 4c), the group I mutants as well as the wild-type protein appeared in two 57 and 52 kDa forms which represent, respectively, the protein precursor and the protein with cleaved C-terminal ecto-domain and covalently linked GPI anchor. Observed incomplete processing may be attributed to protein overexpression as reported previously.[29,30] GPI anchor attachment was less pronounced in the 229R mutant and no precursor processing and GPI linkage was observed in group II mutants.

Treatment with sialidase A (Figure 4e) showed that two proteins from group I mutants – 32Y and 317Y – as well as the wild-type protein sialidase A were sensitive and corresponded to a single zone of ~71 kDa. Partial resistance to sialidase treatment was observed in the 229 R and 236L mutants, which produced two zones of 71 and 65 kDa. Other group II mutants showed the original 71 kDa zone and the processed form of 62 kDa.

Complex deglycosylation with a mixture of all three enzymes (Figure 4d) showed comparable results as for the PNGase F treatment (Figure 4c).

Immunofluorescence

Images of the individual UMOD proteins are shown in Figure 5. The wild-type protein localized on the plasma membrane, with almost no detectable intracellular retention. All the mutant proteins showed granular retention of UMOD in the ER. The ER retention was less pronounced in group I

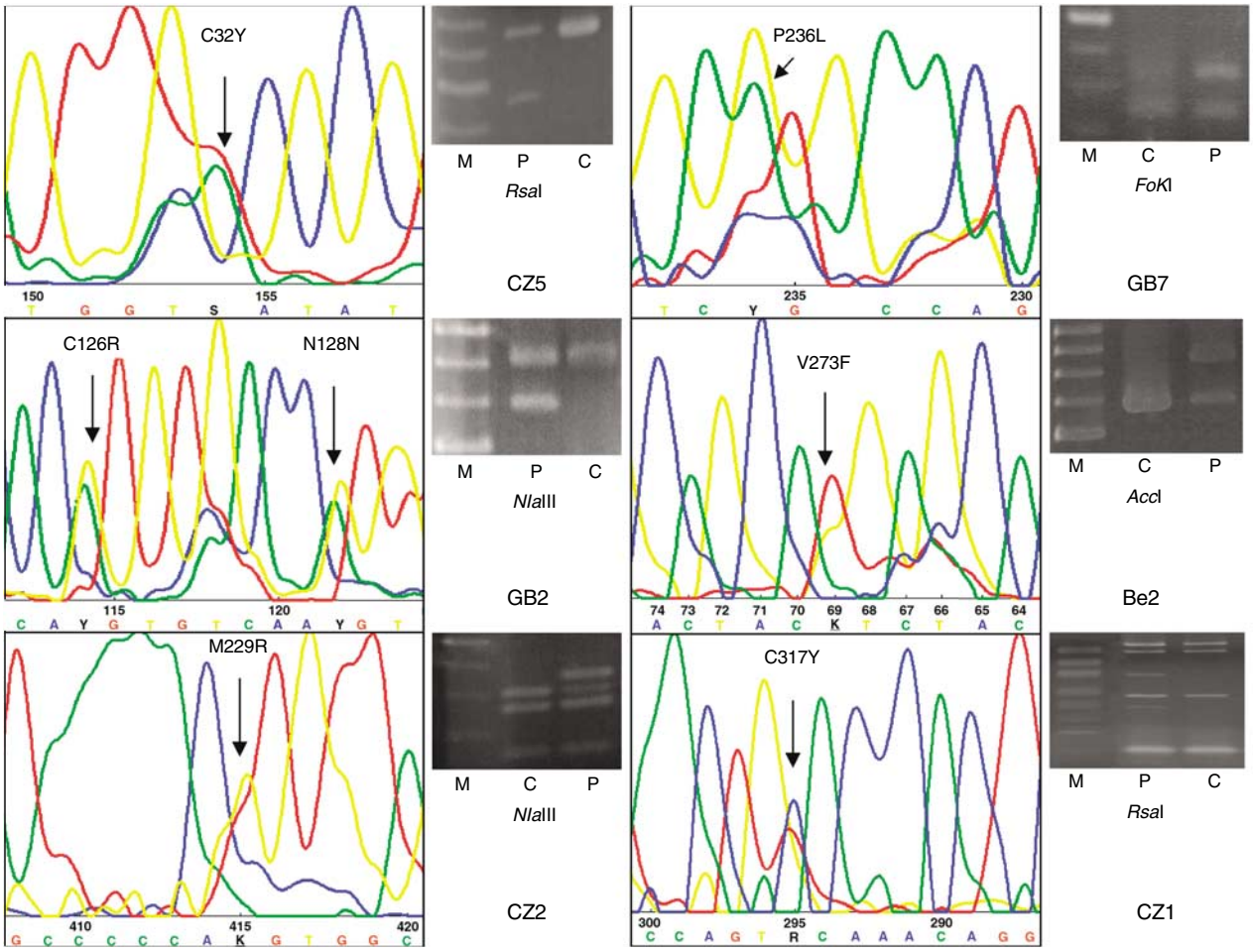

Figure 2 | *UMOD* mutations detected in indicated families and polymerase chain reaction-restriction fragment length polymorphism assays employed in genotyping and mutation analysis. M: size marker standard, P: patient, C: control individual.

mutant proteins, which also showed strong presence on the plasma membrane. The group II mutants showed almost no plasma membrane localization. No significant presence of the proteins in Golgi apparatus was observed (data not shown).

Urinary UMOD analysis

UMOD excretion was investigated in spot urine collected from 71 controls and 96 subjects originating from the 15 affected families. From the 96 subjects, 49 have been classified as affected, based on the clinical and biochemical data obtained. Of those 49 patients, 14 patients have the *UMOD* mutation, 14 patients are from families linked to the *UMOD* region on chromosome 16p11.2 but in whom no *UMOD* mutations have been found, 16 patients are from families in which a linkage has not yet been found, and four patients are from a single family which mapped to the region on chromosome 1q41.[22] One other patient with *UMOD* mutation was investigated after kidney transplantation (T). Qualitative analysis showed the absence or decrease of urinary UMOD excretion in almost all affected individuals. Abnormal UMOD processing has been observed in several individuals, classified as healthy and originated from different families (Figure 6). No co-segregation of the abnormal UMOD processing and disease phenotype has been found.

Quantitative analysis showed that the UMOD excretion was significantly reduced in almost all affected individuals, independent of the linkage groups they belonged to (Figure 7a). Analysis performed separately for each family (Figure 7b) showed that UMOD excretion was reduced in all families except family CZ3. Decreased UMOD excretion was present also in young patients with relatively preserved renal function (Figure 7c). UMOD excretion normalized in a single patient with the *UMOD* mutation after kidney transplantation.

Immunohistochemistry and electron microscopy

Prominent differences in the patterns of UMOD immunohistochemical staining were observed in available kidney tissues. They encompass massive intracellular UMOD accumulation in the patients with *UMOD* mutation, and presence of UMOD in hyaline casts with low intracellular positivity, irregular pattern of UMOD staining or strongly reduced UMOD expression in patients with not yet established molecular defects. Patterns of UMOD staining were correlated and mostly parallel with that of the epithelial membrane antigen (MUC1) (Figure 8).

Table 4 | Nucleotide changes found in *UMOD* genomic sequence

gDNA position	Nucleotide change	Exon/intron	Protein change	dbSNP	Family
UMOD promotor					
−5634	C→C/A				
−5589	G→G/A				
−5494	G→G/A				
−5316	T→T/C				US1
−5074	T→T/C				
−4893	A→A/G				
−4754	G→G/A				
−2531	T→T/C				
−1379	T→T/C				GB3
UMOD-coding sequence					
110	G→G/A	Int 3			
1821	C→C/T	Ex 4	128Asn→Asn		GB2
1959	T→T/C	Ex 4	174Cys→Cys	rs7193058	
2061	G→G/A	Ex 4	208Gln→Gln		
2229	G→G/A	Ex 4	264Val→Val	rs13335818	
2352	G→G/T	Int 4			
2380	T→A	Int 4			
2427	C→C/A	Int 5			CZ3
2793	C→C/A	Int 5			
4662	C→C/T	Int 6		rs4506906	
4779	G→G/A	Int 6			
4805	G→G/A	Int 6			
9192	C→G	Int 7		rs9928757	GB5
9299	T→T/C	Int 7		rs9646256	
9370	C→C/T	Int 7			
9377	C→C/A	Int 7			
13 540	C→C/A	Int 9			

[a]Numbering: initiation codon ATG=1.
Underline values indicate nucleotide changes observed exclusively in indicated families.
Ex, exon; Int, intron; UMOD, uromodulin.

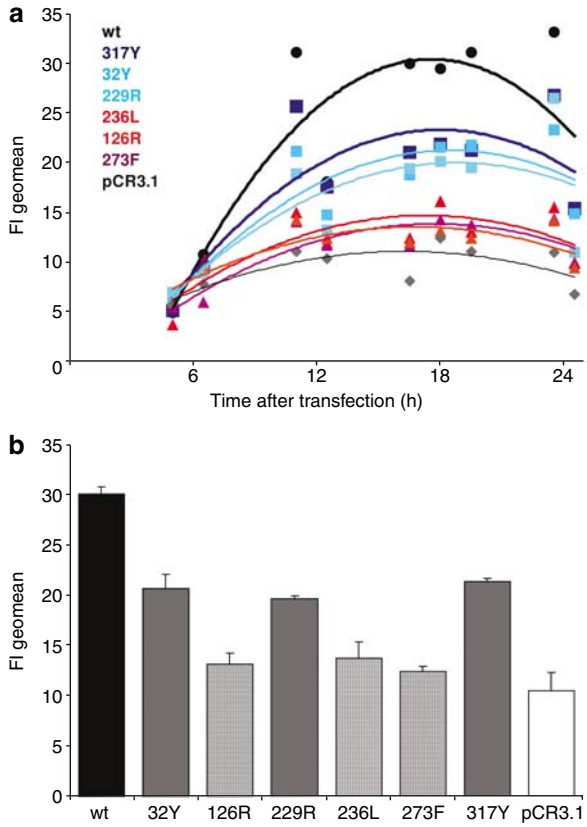

Figure 3 | Fluorescence-activated cell sorter analysis of UMOD-positive AtT-20 cells transfected with pCR3.1 eucaryotic expression vector containing wild-type and identified mutant *UMOD* cDNAs. (**a**) Time course showing saturation of the UMOD plasma membrane exposition in between 18 and 24 h after the transfection. Two groups of mutants, either showing similar dynamics of the plasma membrane exposition as the wild-type protein but with the final amount of the protein significantly reduced (group I mutants, blue lines), and mutants not exposed on the plasma membrane (group II mutants, red lines), are clearly separated. (**b**) The differences in UMOD plasma membrane exposition between wild-type UMOD (black column), group I mutants (gray columns), and group II mutants (dashed columns) measured 18 h after transfection. The values represent means of fluorescence ±s.d. of three transfection experiments carried out in triplicates. The differences between wild-type UMOD, group I mutants, and group II mutants were statistically significant when tested by one-way analysis of variance using Tukey's multiple comparison procedure ($P<0.001$).

Material for ultrastructural studies was available from a single case with M229R UMOD mutation. The tubular epithelium displayed a number of nonspecific changes such as atrophy, hyper regeneration, and increase in dense lysosomal residual bodies. Significant changes related to molecular pathology of the disorder are shown and described in Figure 9. The ER storage material has been identified as an accumulated UMOD protein by immunofluorescence analysis of renal biopsy tissue (Figure 10).

DISCUSSION

FJHN/MCKD is a genetically heterogeneous disease with only a proportion of families having a demonstrable mutation in the *UMOD* gene.

In this work, we characterized in more detail 19 families fulfilling the basic clinical and biochemical criteria of FJHN/MCKD. We completed linkage analysis to three currently known FJHN/MCKD loci – *UMOD* loci on chromosome 16p11.2, MCKD1 loci on chromosome 1q21, and the UAKD loci on chromosome 1q41. The greatest proportion, nine families, showed linkage to the *UMOD* candidate region, the rate of which is comparable with results in several other studies.[8,9,14] Linkage to the UAKD loci on chromosome 1q41 was detected in just a single family and linkage to MCKD1 was not found. Finally, no linkage to any of the above loci was detected in eight families and in a single family, family CZ3, all three loci were even excluded on the LOD = −2 criterion. This result suggests that a second major or several other FJHN/MCKD loci exist and remain to be discovered. Another explanation for such a low detection rate might be false negative results of linkage analysis. In the FJHN/MCKD phenotype, this might be caused by late onset and/or reduced penetrance of the disease,[13,31] phenocopy or by co-occurrence of the disease trait with relatively common phenotypes such as hyperuricemia,[9] gout, or the metabolic syndrome.[32] However, analysis of the *UMOD* genomic sequence showed the false negativity of linkage analysis only in a single family GB7. Interestingly, *UMOD* mutations were found in five but

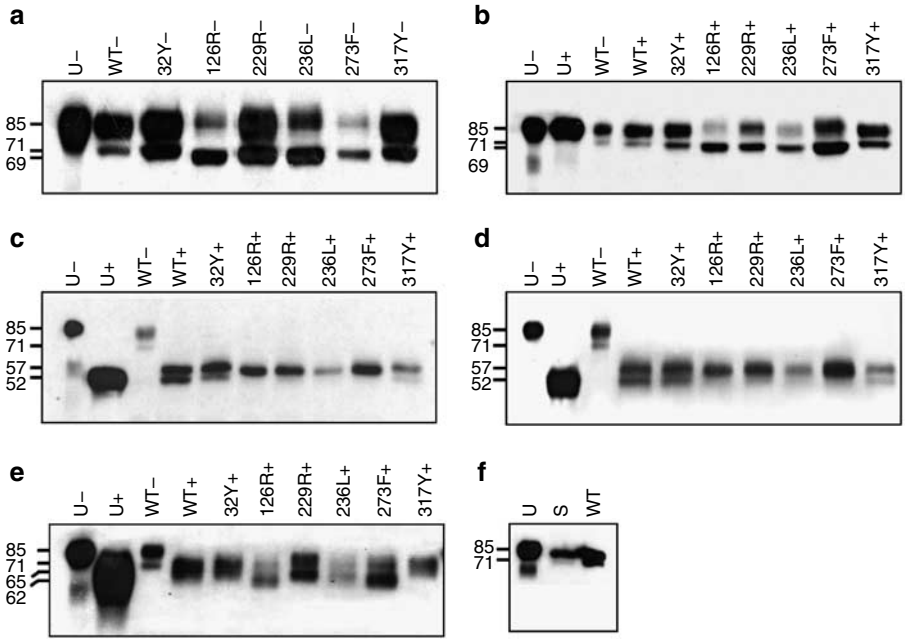

Figure 4 | Western blot analyses of wild-type (WT) and individual mutated UMOD-expressing AtT-20 cell lyzates treated by various glycosidases. Lyzates of transfected cells, (**a**) harvested 24 h after transfection, were treated by (**b**) *O*-glycanase, (**c**) PNGase F, (**e**) sialidase A, and (**d**) mixture of PNGase F, *O*-glycanase, and sialidase. Panel (**f**) shows Western blot analysis of lyzates of stable (S) and transiently (WT) UMOD-expressing cell lines. Uromodulin isolated from urine (U) was used as a control; + indicates treatment and − indicates no treatment with corresponding glycosidase. Molecular weights are given in kilodaltons on the left-hand side of the individual panels. The molecular weight calibration curve was constructed by plotting decadic logarithm of molecular weights versus distance of corresponding bands of the protein molecular weight marker (Precision Plus Protein Kaleidoscope Standards, Biorad) from the upper edge of the SDS-PAGE gel after blotting. Molecular weights of different UMOD glycoforms were calculated from their distances using logarithmic regression equation.

not in the other four families originally linked to *UMOD* candidate region on chromosome 16p11.2. This finding may be explained by false positivity of the linkage analysis that has arisen from the small number of investigated individuals or indicates the existence of other disease gene located in the *UMOD* candidate region. The other explanation may be undetected mutations in *UMOD* promoter sequence or the existence of synonymous exonic mutations and/or intronic mutations affecting proper *UMOD* mRNA processing. We found several such 'private mutations' in the promoter sequence in families US1 and GB3 but their potential pathogenic effect has not yet been further investigated. Overall, only six disease-causing mutations in the *UMOD* gene were identified in 19 FJHN/MCKD families. Such a low detection rate is in agreement with at least two similar extensive studies[8,9] and further confirms the considerable degree of genetic heterogeneity of the FJHN/MCKD phenotype.

Functional consequences of *UMOD* mutations

From the identified mutations, three mutations have been already reported in other families. Mutation C126R was found in family GB2, in Italian family F5,[9] and an Austrian family 13/00,[6] which is a branch of family GB2. Mutation C317Y was found in Czech family CZ1 and in an Italian family MCKD no. 1.[7] Mutation P236L was found in GB7 and in the Japanese family no. 1.[10] Three identified mutations, C32Y, M229R, and V273F are novel. To prove their pathogenity, we cloned all the mutations and characterized transiently expressed mutant proteins. All the mutant proteins differed from the wild-type protein in their ability to reach the exoplasmic face of the plasma membrane and according to it they clustered into two groups. Group I mutants showed reduced ability and group II mutants were not able to reach the plasma membrane. The ability of the protein to reach the plasma membrane was determined by GPI modification. GPI-modified proteins (group I mutants) may exit endoplasmic reticulum, enter secretory pathway and reach the plasma membrane. In these mutants, the associated pathogenic mechanism may thus be related to impaired intracellular trafficking, decreased ability of the protein to be properly internalized and exposed on the exoplasmic face of the plasma membrane, or defective assembly of UMOD filaments. In contrary, mutants lacking GPI (group II mutants) cannot exit and remain retained within ER lumen, which leads to marked expansion of the organelle, attenuation of the translation of other polypeptides, activation of the stress signaling pathway, and progressive tissue damage.[30] Both mechanisms are compatible with a concept of autosomal dominant negative effect of the disease. In the group I mutants, both the wild-type and misfolded mutant protein may be trapped together in transport cargo vesicles where their co-occurrence may delay or hamper intracellular

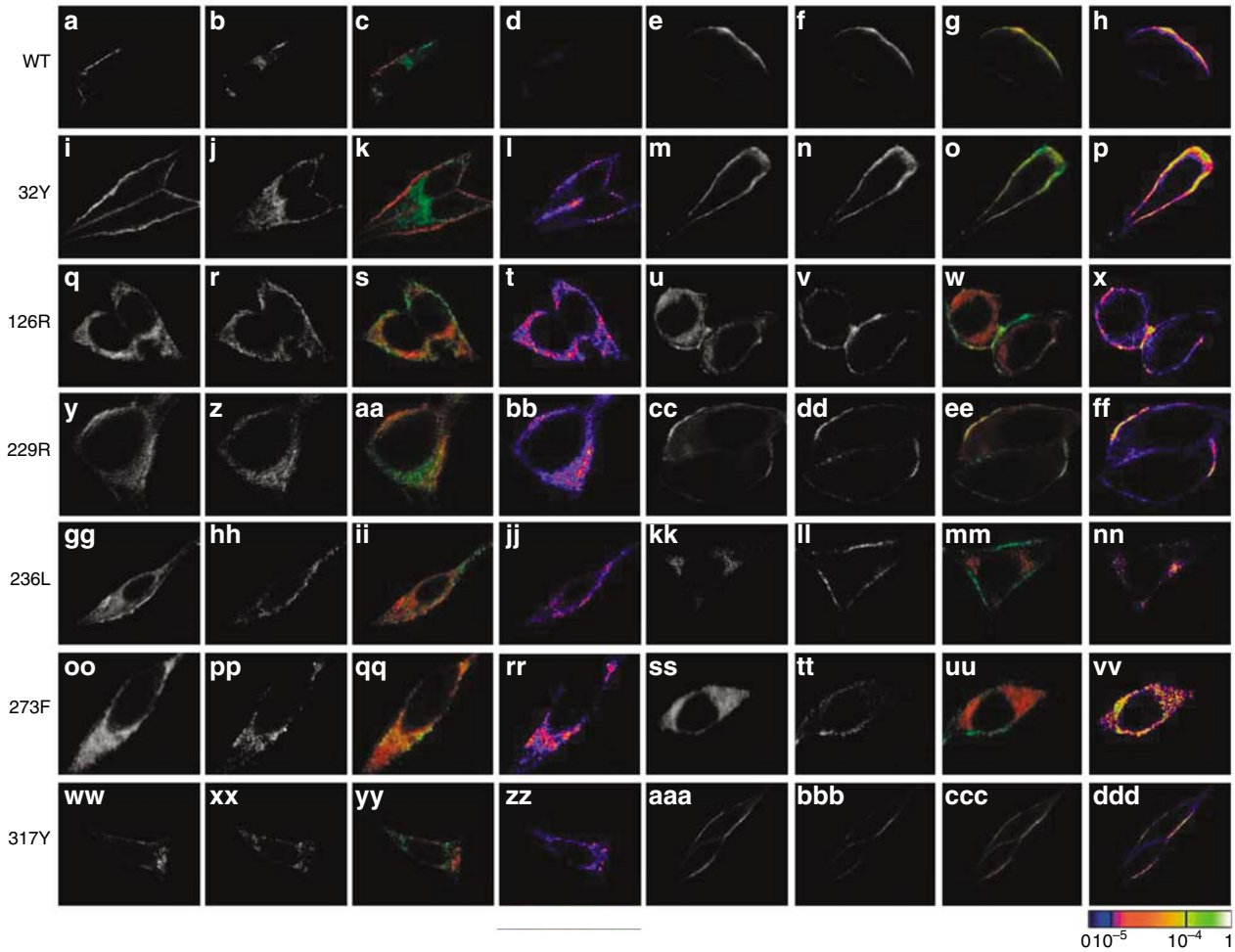

Figure 5 | Cellular localization of wild-type UMOD and individual UMOD mutants in permeabilized AtT-20 cells studied 18 h after transfection. Columns (**a, i, q, y, gg, oo, ww, l, m, u, cc, kk, ss, aaa**) UMOD; columns (**b, j, r, z, hh, pp, xx**) PDI as a marker of ER; column (**f, n, v, dd, ll, tt, bbb**) pan-Cadherin as a marker of plasma membrane. Column (**c, k, s, aa, ii, qq, yy**) show merged signals of individual UMOD proteins (red fluorescence) with the markers of ER (green fluorescence). In column (**d, l, t, bb, jj, rr, zz**), the resulting colocalization map of UMOD and PDI is shown. Column (**g, o, w, ee, mm, uu, ccc**) show merged signals of individual UMOD proteins (red fluorescence) with the marker of plasma membrane (green fluorescence). In column (**h, p, x, ff, nn, vv, ddd**), the resulting colocalization map of UMOD and pan-Cadherin is shown. Wild-type UMOD localized exclusively on the (**g, h**) plasma membrane, with only minor presence in the (**c, d**) ER. (**k, s, aa, ii, qq, yy** and **l, t, bb, jj, rr, zz**) All the mutant proteins show retention of UMOD in the ER. The ER retention is less pronounced in the properly GPI-modified group I mutants 32Y (**k, l**), and 317 Y(**yy, zz**), which show also strong presence on the plasma membrane (**o, p** and **ccc, ddd**), respectively. Only partly GPI-processed 229R mutant (row **y–ff**), and GPI-unprocessed 126R mutant (row **q–x**) show irregular plasma membrane localization (**ee, ff** and **w, x** respectively). The transport compromised group II mutants 236L (row **gg–nn**) and 273F (row **oo–vv**) show almost no plasma membrane localization (**mm, nn** and **uu, vv** respectively).

trafficking process or lateral transmembrane transport as in several other kidney diseases.[33] Another alternatives might be that the presence of the mutant protein on the cell surface hampers proper copolymerization and assembly of UMOD filaments,[34] which then affects the proper biological function(s) of UMOD on the plasma membrane. In the group II mutants, the disease mechanism might be different. The mutant protein is probably retained and accumulates gradually in the ER. The accumulation of unfolded proteins in the ER leads to marked expansion of the organelle, attenuation of the translation of other polypeptides, activation of the stress signaling pathway, and progressive tissue damage.[35] Two questions however remain to be answered. First, to what extent the results of *in vitro* studies correlate with the real situation in kidney tissues of affected individuals and second, whether any particular phenotypic patterns might be assigned to individual UMOD mutant groups. Such a correlation might have been done only for the mutation 229R. According to the expression studies, this mutation seems to have both the suggested pathogenic effects. The protein should reach to a certain extent the plasma membrane but it should also be less efficiently GPI modified and retained in the ER. This possibility corresponds well with the immunohistochemistry and electron microscopy investigations of the kidney tissue available from the patient. Eventual genotype-specific phenotypic differences cannot be judged easily since only a small number of families and inadequate clinical data are currently available. More

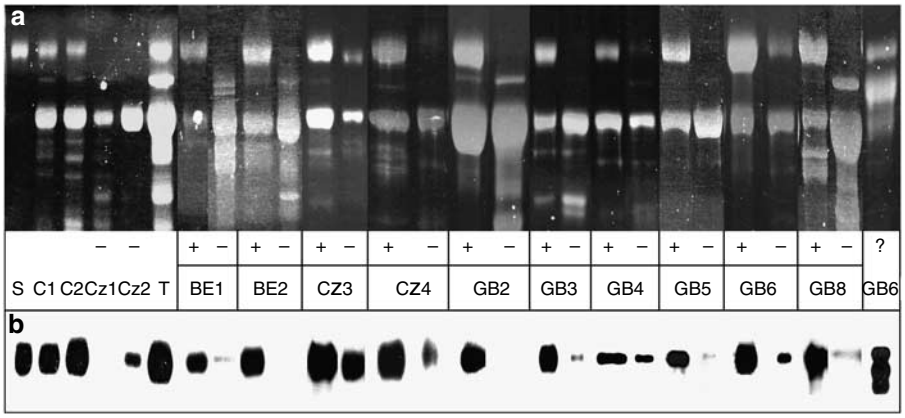

Figure 6 | Qualitative analysis (SDS-PAGE and Western blot) of urinary UMOD in a single affected proband (−) and healthy individual (+) from UAKD families showing the absence or significant reduction in urinary UMOD excretion. S: uromodulin standard isolated from control urine, C: control urines, T: urine from patient with UMOD mutation after successful kidney transplantation ?: abnormal UMOD processing that has been observed in several healthy individuals from various families.

work in this direction is warranted since different pathogenic mechanisms might be targeted more effectively by different therapeutic approaches.[36]

Defects in UMOD biology seems to be common to the pathogenesis of FJHN/MCKD

The link between UMOD mutations, intracellular protein aggregation, and absence of the protein in urine has been shown in several studies.[7,9,37] However, not much information is available on UMOD excretion in FJHN/MCKD patients having no *UMOD* mutation. Analysis in a single such family showed normal UMOD excretion[9] and it has been suggested that a drop in the UMOD urinary excretion is specific only for cases with *UMOD* mutations.[38] Our investigations however showed that UMOD excretion was significantly decreased in all but one family. Decreased UMOD excretion could be considered as being secondary to renal disease.[39] While this might be true we favor the explanation that our findings reflect and highlight the central role of UMOD dysfunction in the development of common FJHN/MCKD symptoms. This central role might be attributed to the absence of proper UMOD function on the plasma membrane and/or in the urine, as this factor seems to be common to all the cases we have had the opportunity to investigate. The absence of UMOD properly expressed on the plasma membrane might result from different molecular mechanisms such as reduced gene expression resulting from a mutation of transcription factor as demonstrated in the case of the *HNF1-β* mutation[23,40] or in hypothyroidism,[41] from protein mistargeting, inability of the protein to be properly GPI-anchored, from gradual gene expression silencing resulting from aberrant developmental processes or from aberrant cellular differentiation or proliferation.[42]

UAKD

Possible pathogenic mechanisms linking *UMOD* mutations with characteristic disease symptoms have been discussed recently.[43] Hyperuricemia in UAKD results from the underexcretion of uric acid. This feature usually appears at an early age, well before the renal disease becomes apparent, so it seems that hyperuricemia is somehow directly linked to UMOD dysfunction. Our data from 36 UAKD patients show positive correlation between urinary urate and urinary UMOD concentrations ($r = 0.62$; $P < 0.0001$), and this trend has been observed also in 113 healthy individuals ($r = 0.18$; $P \leqslant 0.05$). As minor *UMOD* expression has been found also in proximal tubule cells,[44] abnormal urate handling and UMOD dysfunction linked through enhanced urate reabsorption in the proximal tubule is a distinct possibility. Another mechanism linked to hyperuricemia might be a dysfunction of the UMOD containing water barrier on the apical membrane of the loop of Henle cells, which may result in nonspecific transcellular transport of urate in this segment. Defects in the secretion, or enhanced postsecretory reabsorption of urate linked to UMOD absence in the distal convoluted tubule or collecting duct is yet another possibility.

A common feature present in UAKD patients is also a loss of urine concentrating efficiency.[31,43] It has been suggested that low urine osmolality may be attributed to dysregulation of ion transport and electrolyte homeostasis. We hypothesize that decreased urine concentrating efficiency might result from the absence of released UMOD in both, the distal convoluted tubule and the collecting duct. UMOD is fundamental in cast formation, which takes place in the late section of the distal tubules and the early section of the collecting duct. Absence of UMOD may thus prevent cast formation, enhance urine flow, impair water reabsorption, and result in low urine osmolality. Abnormality in urine flow and dysregulation of major distal tubule transporters in UMOD−/− mice[45] supports this hypothesis.

To conclude, in our work we have shown that various genetic defects and mechanisms hamper various steps in UMOD biology, which probably leads to the development of

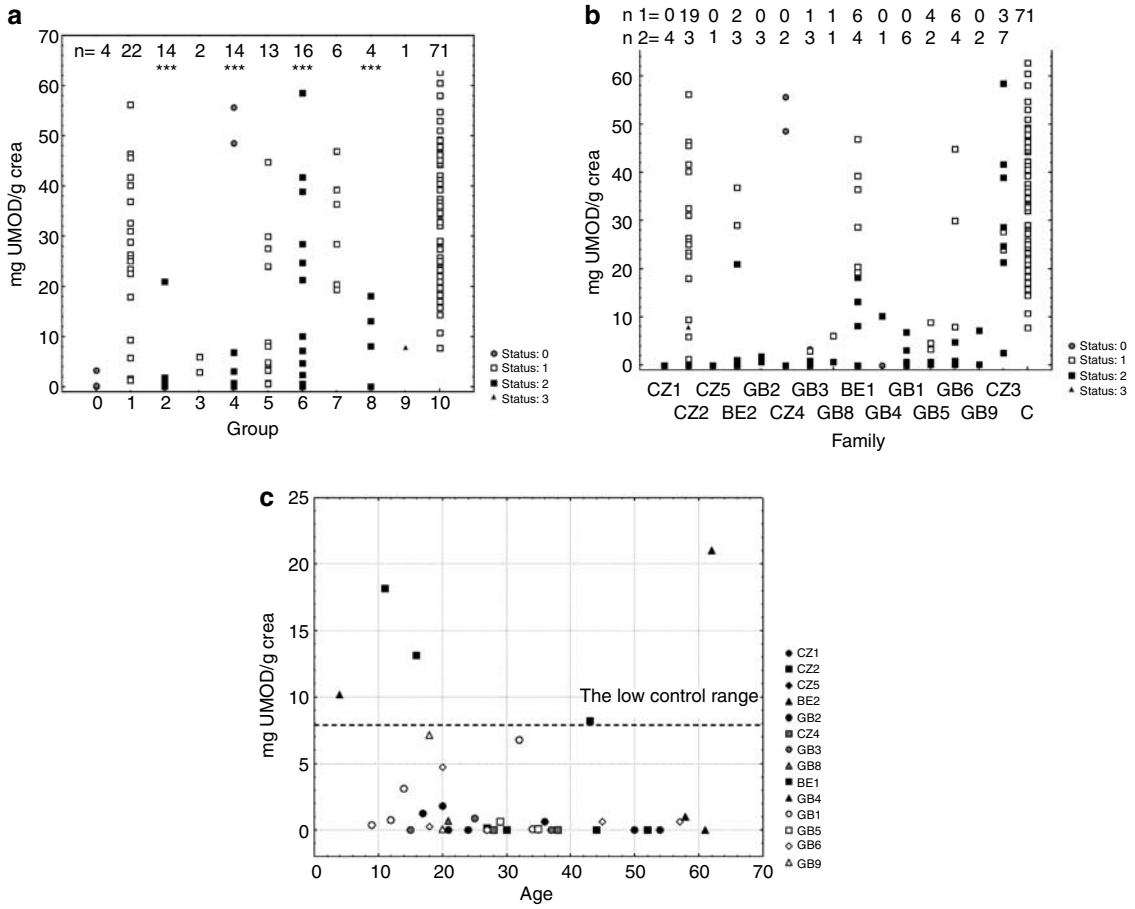

Figure 7 | Quantitative analysis (enzyme-linked immunosorbent assay) of urinary UMOD excretion. (**a**) Data plotted for the individual linkage groups. 0: individuals of unknown status; 1: healthy individuals and 2: affected individuals from families with the *UMOD* mutation; 3: healthy individuals and 4: affected individuals from families linked to the *UMOD* candidate region on chromosome 16p11.2 but in which no mutation in the *UMOD* gene has been detected; 5: healthy individuals and 6: affected individuals from families in which no linkage to any of UAKD loci has been detected; 7: healthy individuals and 8: affected individuals from a family linked to UAKD loci on chromosome 1q41; 9: a patient with UMOD mutation after successful kidney transplantation; 10: controls. The number of individuals investigated in each of the groups is indicated above corresponding columns. *P*-values (*t*-test) correspond to the comparisons between indicated group and controls; ***$P < 0.001$. (**b**) The same results of quantitative urinary UMOD excretion plotted for individual families and showing reduction of UMOD excretion in all families with an exception of CZ3. The number of individuals investigated in each group is indicated above the corresponding columns; n 1 and n 2 denotes the number of healthy and affected individuals, respectively. Status 0 represents an unknown phenotype, status 1 and 2 represent healthy and affected individual, respectively. Status 3 represents a patient with UMOD mutation after successful kidney transplantation. (**c**) Decreased UMOD excretion is present also in young patients with relatively preserved renal function. It is suggestive that in the reported families the UMOD dysfunction precedes the onset of renal insufficiency. Black symbols denote patients from families with *UMOD* mutations. Gray symbols denote patients from families with no *UMOD* mutations but showing linkage to UAKD-associated loci. Black/white symbols denote patients from families in which no linkage to any of UAKD loci has been detected. Patients from family CZ3 showing normal UMOD excretion are not included in this figure. Control values of UMOD excretion are reported in Table 1 and its distribution is shown in panels **a** and **b**.

common FJHN/MCKD phenotype. This finding supports the term of UAKD[5,22] as the most appropriate for the FJHN/MCKD designation. Given the frequency of urate abnormalities, an alternative designation might be 'familial urate–uromodulin nephropathy'.

UMOD urinary excretion analysis with subsequent *UMOD* sequencing is currently the primary diagnostic test in UAKD patients. As suggested previously[9] and clearly documented here in family CZ5, this investigation should be undertaken even in sporadic cases, in the absence of family history as *de novo* mutations do appear. However, as the protein has tendency to aggregate, a caution should be exercised in interpretation of UMOD quantitative data.[37,46] Qualitative Western blot analysis represents at least in our hands the preferred method for extensive urinary UMOD testing which has the potential to identify more UAKD families without *UMOD* mutations. In these families, linkage analysis to already defined loci or alternatively, whole genome scans may be performed to confirm and narrow the existing loci, or to reveal not yet identified UAKD loci. Identification and characterization of other UAKD loci may help to clarify the exact biological roles of UMOD, provide better diagnostic techniques, and finally suggest potential therapeutic targets and therapeutic approaches.[36]

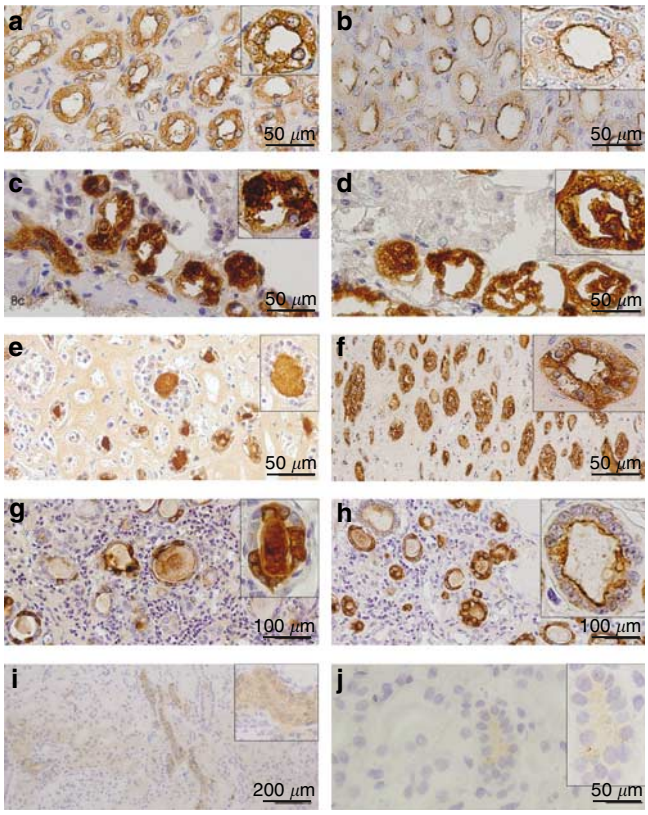

Figure 8 | Immunohistochemical analysis of UMOD and MUC1 in kidney biopsies. In control tissue, (**a**) UMOD shows diffuse cytoplasmic staining with maximal intensity on the apical membranes and (**b**) MUC1 is expressed almost exclusively on the apical membrane of the cells of the ascending limb of the loop of Henle. The tissue of patient with the *UMOD* mutation shows (**c**) massive intracellular accumulation of UMOD and (**d**) abundant MUC1 presence with strong uniform intracellular positivity. In a case from family GB3 linked to the *UMOD* region on chromosome 16p11.2 but in which no *UMOD* mutation has been found, shows (**e**) UMOD to be present in hyaline casts with low intracellular positivity and (**f**) normal or variable intracellular increase of MUC1 exceeding this of UMOD. A case from family GB6, in which no linkage to any of the UAKD loci has been found shows (**g**) an irregular pattern of UMOD staining and (**h**) normal or close to normal expression of MUC1. In three patients from a family linked to 1q41, (**i**) UMOD and (**j**) MUC1 expression is strongly reduced and both proteins are present in the form of tiny intracellular granules.

MATERIALS AND METHODS

Patients

In total, 19 families were enrolled in this study. Five families are from the Czech Republic. Pedigrees of families CZ1, CZ2, and CZ3 have been reported (A, B, and C, respectively) previously;[13] CZ4, CZ5, and a single family from the USA (US1) are reported here for the first time. Ten families are from Great Britain (GB1–GB10) and two families are from Belgium (BE1, BE2).[15] The single family is from Finland (MCKD family 6).[18]

Biochemical investigations

Collected random spot urine samples were stored at −80°C. Urine total protein, creatinine, uric acid, magnesium, calcium, phosphate, sodium, potassium, chloride, osmolality, and qualitative and quantitative UMOD excretion were determined as previously described.[22]

Genotyping and linkage analysis

For MCKD/FJHN locus on chromosome 16p11.2, a set of 13 microsatellite markers D16S499–D16S501–D16S3056–D16S3041–D16S3036–D16S3046–D16S403–D16S412–D16S3130–D16S417–D16-S420–D16S3113–D16S401; for MCKD1 locus on chromosome 1q21, a set of three microsatellite markers D1S1153–D1S2624–D1S2125; and for UAKD locus on chromosome 1q41, a set of 11 markers GATA31D05–D1S373–D1S2773–D1S245–D1S2703–D1S490–D1S1644–D1S1656–D1S2649–D1S2850–D1S2670 were used. Genotyping and linkage analysis were performed as previously described.[15,22]

UMOD gene analysis

Genomic organization, upstream promoter region sequence, and genomic sequence of the *UMOD* gene were obtained using pairwise BLASTN comparison of the *UMOD* cDNA sequence with the corresponding genomic sequences. Primers for polymerase chain reaction amplification and sequencing were designed using software Oligo (National Biosciences, Plymouth, MN, USA). Genomic fragments covering the promoter and all of the exons and intron–exon boundaries were polymerase chain reaction amplified and sequenced as previously described[47] in a single proband and unaffected individual in each family.

UMOD cDNA expression constructs

UMOD cDNA was prepared from kidney cDNA using primers UcDNA1U and UcDNA2L, cloned into pCR4-TOPO sequencing vector (Invitrogen, Paisley, UK) and introduced into the *Escherichia coli* TOP 10'F strain (Invitrogen, Paisley, UK). Mammalian expression construct UcDNAwt/pCR3.1 was prepared by subcloning of the UcDNAwt/pCR4-TOPO insert into pCR3.1 vector (Invitrogen, Paisley, UK) using *Eco*RI restriction sites. Mutated constructs UcDNA229R/pCR3.1, UcDNA126R/pCR3.1, and UcDNA236L/pCR3.1 were prepared by cloning of mutation bearing polymerase chain reaction fragments, first into UcDNAwt/pCR4-TOPO construct (UMODE4,5: 51980U and Cy5ex4,5-A primers, *Sac*I a BstAPI restriction sites), and then into pCR3.1 vector (Invitrogen, Paisley, UK), using *Eco*RI restriction sites as described above.

Mutated constructs UcDNA32Y/pCR3.1, UcDNA273F/pCR3.1, and UcDNA317Y/pCR3.1 were prepared by site-directed mutagenesis of UcDNAwt/pCR3.1 construct (GeneTailor kit, Invitrogen, Paisley, UK). All the primer sequences are available upon request.

Cell culture and transfection experiments

AtT-20 pituitary cells were maintained in DMEM high glucose medium supplemented with 10% (vol/vol) fetal calf serum, 100 U/ml penicillin G, and 100 μg/ml streptomycin sulfate (PAA Laboratories GmbH, Pashing, Austria). Cells were used at 80% confluence. Transfection was carried out with 4 μg of DNA using Lipofectamine 2000™ (Invitrogen, Paisley, UK).

Flow cytometry

AtT-20 cells were seeded in six-well tissue culture plates (BD Falcon, Palo Alto, CA, USA). Following 24-h incubation, the cells were transfected and harvested at the indicated time after the transfection. 2×10^5 cells were washed, stained for 30 min with 1.5 μg of fluorescein isothiocyanate-labeled (Fluorescent Labelling Kit, Roche, Prague, Czech Republic) anti-UMOD – rabbit polyclonal IgG (Biogenesis, Pool, UK), washed and fixed in 2% paraformaldehyde. Fluorescence was measured using FACSCalibur flow cytometer and analyzed using the Cell Quest software version 3.3 (Becton Dickinson, San Jose, CA, USA). Cell-surface expression of UMOD was quantified as the geomean of the fluorescence of gated fluorescein isothiocyanate-positive cells.

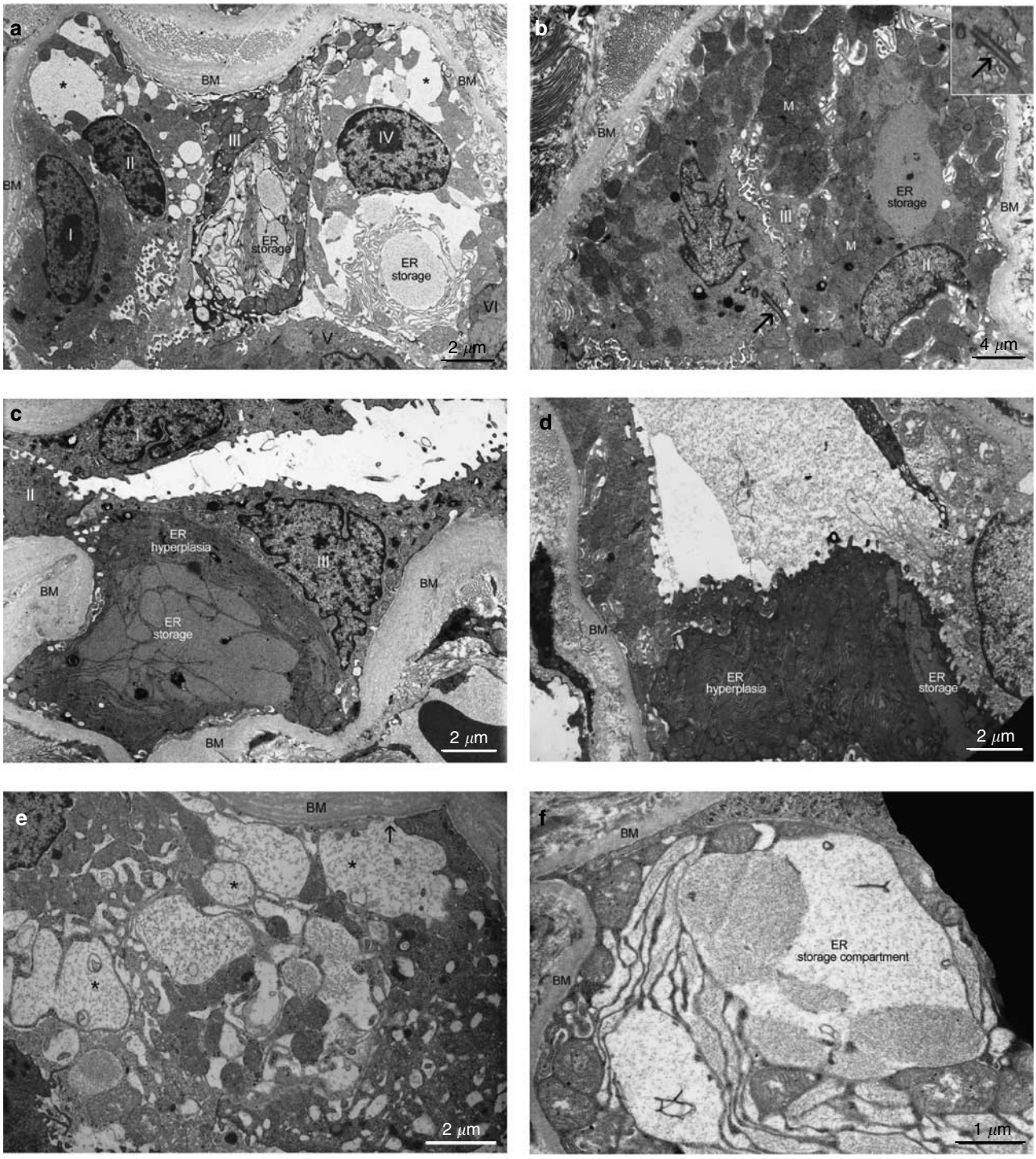

Figure 9 | Ultrastructural changes in renal tubules compatible with the ascending loop of Henle prepared from the kidney biopsy from a patient with the M229R UMOD mutation. Individual cells are labeled with Roman numerals, ER: endoplasmic reticulum, BM: basal membranes, M: mitochondria, *: distended basal invaginations. (**a**) Considerably distended basal invagination of many tubules projected into the cell interior. (**b**) Thickened and partly multilayered basement membrane with increase in the number of mitochondria, which were generally rich in the inner membrane system. Cilia is shown by arrow and enlarged in the insert. (**c**, **d**) Abundant slender rough ER cisternae arranged in slightly curved or whirled stacks present in flat tubular epithelia and in those exhibiting expansion of ER with amorphous moderately dense content ranging from slight to massive distension. (**e**) Detail of distension of the basal cisternae with an arrow pointing to their communication with the extracellular space. (**f**) Detail of the ER storage areas either bulging into the apical pole luminally or facing the basolateral pole.

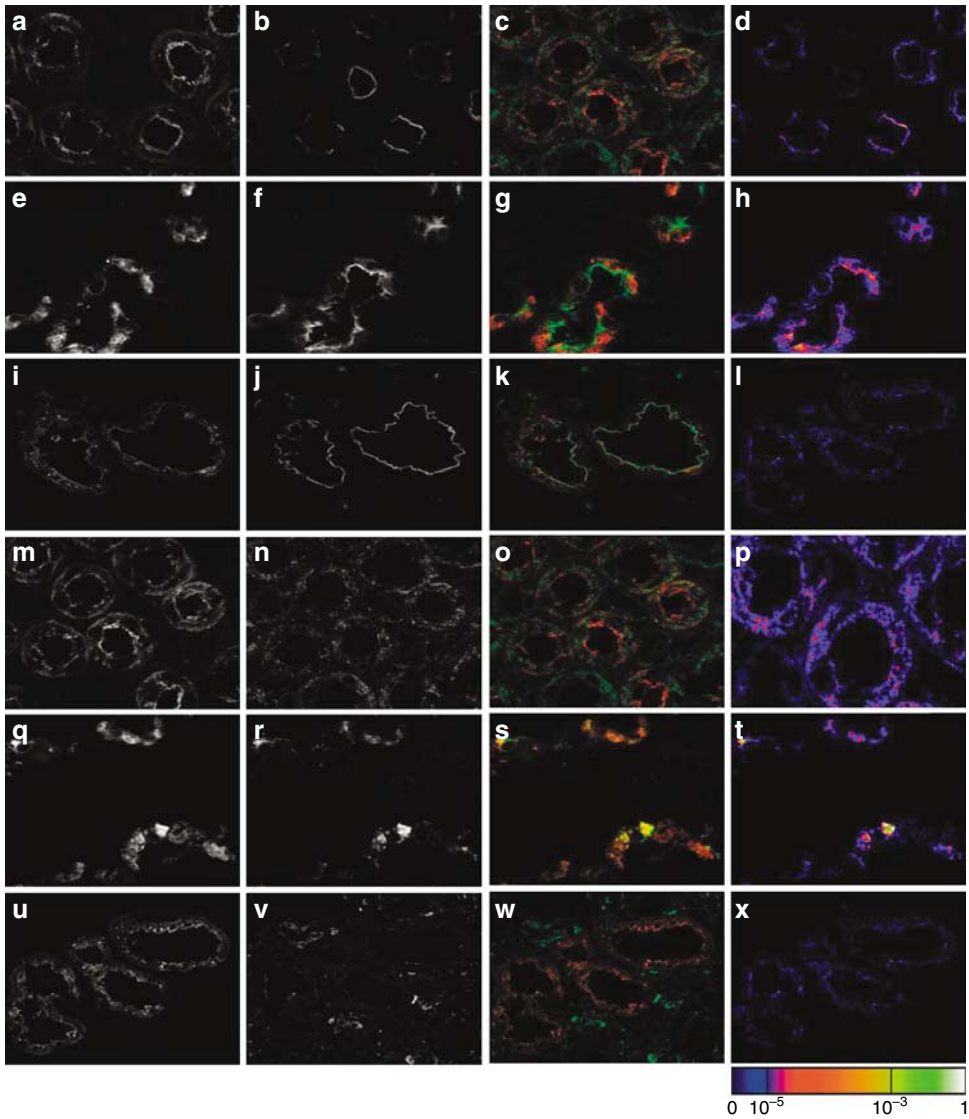

Figure 10 | Cellular localization of the UMOD in the renal biopsy tissue from control (rows a–d, m–p), from patient with the M229R UMOD mutation (rows e–h, q–t), and from patient with no *UMOD* mutation (rows i–l, u–x). In control, (**a**) UMOD is clearly present on apical membrane of the ascending limb of the loop of Henle cells as is the plasma membrane marker (**b**) MUC1. In patient with the M229R UMOD mutation, both (**e**) UMOD and (**f**) MUC1 show diffuse intracellular staining pattern suggesting decreased efficiency in targeting of membrane cargo proteins into plasma membrane. In patient with no *UMOD* mutation, (**i**) UMOD shows diffuse intracellular staining pattern as in the case with UMOD mutation, but (**j**) MUC1 expression is clearly normal. (**c, g, k**) Merged fluorescence signals of UMOD (red) and MUC1 (green), and (**d, h, l**) colocalization maps employing overlap coefficient values are shown for control, patient with the M229R UMOD mutation and patient with no *UMOD* mutation, respectively. In patient with the M229R UMOD mutation, the intracellular localization of (**q**) UMOD was assigned almost exclusively into (**r**) ER as seen by fluorescence signal merge of UMOD (red) with (**s**) ER marker PDI (green) and the corresponding (**t**) colocalization map. The degree of UMOD signal retention in ER is demonstrated by the overlap coefficient value (note the scale of the lookup tables, compare to (**p**), and see the massive ER storage in Figure 9). In patient with no *UMOD* mutation, the intracellular localization of (**u**) UMOD could not be attributed to (**v**) ER, as seen by fluorescence signal merge of UMOD (red) with (**w**) ER marker PDI (green) and the (**x**) corresponding colocalization map. In this case, the defect seems to affect either proper UMOD internalization into plasma membrane or inefficient targeting and/or processing of UMOD in ER (compare colocalization maps for (**p**) control and (**x**) patient).

SDS-PAGE and Western blotting analysis

Harvested cells were resuspended in phosphate-buffered saline containing Protease inhibitor coctail (Sigma, Prague, Czech Republic) and sonicated. UMOD was detected as described previously.[22]

Deglycosylation experiments

Deglycosylation experiments were performed on cell lyzates using the GlycoPro™ enzymatic deglycosylation kit (ProZyme Inc., San Leandro, CA, USA). Deglycosylated products were analyzed by sodium dodecyl sulfate-polyacrylamide gel electrophoresis (SDS-PAGE) and Western blot as described above.

Immunofluorescence

For immunofluorescence, 6.5×10^4 of AtT-20 cells were grown on 70 mm^2 glass chamber slides (BD Falcon – 4Chamber Polystyrene Vessel Tissue Culture Treated Glass Slide) for 24 h and transfected as described above. At 18 h after the transfection, the cells were fixed with 100% methanol at −20°C, washed, blocked with 5% FCS

and incubated for 1 h at 37°C with primary antibodies: rabbit Anti-Human THP polyclonal antibodies (Biogenesis, Poole, UK) or Anti-Human THP mouse IgG2b monoclonal antibodies (Cedarlane, Hornby, Ontario, Canada) for UMOD detection; anti-PDI – mouse monoclonal IgG1 (Stressgen, San Diego, CA, USA) for ER localization; anti-GS28 mouse monoclonal IgG (Stressgen, San Diego, CA, USA) for Golgi localization, and anti-pan Cadherin rabbit polyclonal IgG (Abcam, Cambridge, UK) for plasma membrane localization. For fluorescence detection, secondary antibodies – Alexa 568 goat anti-rabbit IgG and Alexa 488 goat anti-mouse IgG (Molecular Probes, Invitrogen, Paisley, UK) were used. Prepared slides were mounted in fluorescence mounting medium Immu-Mount (Shandon Lipshaw, Pittsburgh, PA, USA) and analyzed by confocal microscopy.

Image acquisition and analysis

XYZ images sampled according to Nyquist criterion were acquired using Nikon Eclipse E800 microscope equipped with C1 confocal head, Nikon PlanApo objective (60X, N.A.1.40), 488 and 543 nm laser lines, and 515 ± 15 and 590 ± 15 nm band pass filters. Images were deconvolved using classic maximum likelihood restoration algorithm in the Huygens Professional Software (SVI, Hilversum, The Netherlands).[48] The colocalization maps employing single pixel overlap coefficient values ranging from 0 to 1[49] were created in the Huygens Professional Software. The resulting overlap coefficient values are presented as the pseudocolor whose scale is shown in corresponding lookup tables.

Immunohistochemistry studies

Formaldehyde- or ethanol-fixed kidney samples were analyzed. Immunodetection of UMOD was performed as previously described.[22] Immunodetection of mucine 1 (MUC1, epithelial membrane antigen) was carried out using anti-MUC1 monoclonal antibody (DAKO, Carpinteria, CA, USA).

Electron microscopy

Renal biopsy specimen was fixed with 4% paraformaldehyde (PFA) in 0.1 M phosphate buffer for 30 min and by buffered 1% OsO_4 for 2 h, dehydrated and embedded into Epon. Thin sections were double contrasted with uranyl acetate and lead nitrate. Photographs were obtained on a TESLA 500 electron microscope.

ACKNOWLEDGMENTS

We thank Gert Matthijs, Elly Pijkels, Bernard Kaplan, Sirpa Ala-Mello, Miroslav Ryba for their efforts in collection of biological materials and patient's data; Jana Sovová for performing the immunohistochemical analysis; Květa Pelinková and Slávka Vaníčková for performing the clinical biochemistry analyses; and Stewart Cameron for critical reading of the manuscript. This work was supported by grant 5NE/7046 from the Grant Agency of the Ministry of Health of the Czech Republic and grant 203 200 from the Grant Agency of Charles University of Prague. Institutional support was provided by grant MSM0021620806 from the Ministry of Education of the Czech Republic.

REFERENCES

1. Duncan H, Dixon A. Gout, familial hyperuricaemia and renal disease. *Q J Med* 1960; **29**: 127–136.
2. Cameron JS, Moro F, Simmonds HA. Gout, uric acid and purine metabolism in paediatric nephrology. *Pediatr Nephrol* 1993; **7**: 105–118.
3. Goldman SH, Walker SR, Merigan Jr TC *et al.* Hereditary occurrence of cystic disease of the renal medulla. *N Engl J Med* 1966; **274**: 984–992.
4. Scolari F, Puzzer D, Amoroso A *et al.* Identification of a new locus for medullary cystic disease on chromosome 16p12. *Am J Hum Genet* 1999; **64**: 1655–1660.
5. Hart TC, Gorry MC, Hart PS *et al.* Mutations of the UMOD gene are responsible for medullary cystic kidney disease 2 and familial juvenile hyperuricaemic nephropathy. *J Med Genet* 2002; **39**: 882–892.
6. Turner JJ, Stacey JM, Harding B *et al.* UROMODULIN mutations cause familial juvenile hyperuricemic nephropathy. *J Clin Endocrinol Metab* 2003; **88**: 1398–1401.
7. Rampoldi L, Caridi G, Santon D *et al.* Allelism of MCKD, FJHN and GCKD caused by impairment of uromodulin export dynamics. *Hum Mol Genet* 2003; **12**: 3369–3384.
8. Wolf MT, Mucha BE, Attanasio M *et al.* Mutations of the uromodulin gene in MCKD type 2 patients cluster in exon 4, which encodes three EGF-like domains. *Kidney Int* 2003; **64**: 1580–1587.
9. Dahan K, Devuyst O, Smaers M *et al.* A cluster of mutations in the UMOD gene causes familial juvenile hyperuricemic nephropathy with abnormal expression of uromodulin. *J Am Soc Nephrol* 2003; **14**: 2883–2893.
10. Kudo E, Kamatani N, Tezuka O *et al.* Familial juvenile hyperuricemic nephropathy: detection of mutations in the uromodulin gene in five Japanese families. *Kidney Int* 2004; **65**: 1589–1597.
11. Rezende-Lima W, Parreira KS, Garcia-Gonzalez M *et al.* Homozygosity for uromodulin disorders: FJHN and MCKD-type 2. *Kidney Int* 2004; **66**: 558–563.
12. Tinschert S, Ruf N, Bernascone I *et al.* Functional consequences of a novel uromodulin mutation in a family with familial juvenile hyperuricaemic nephropathy. *Nephrol Dial Transplant* 2004; **19**: 3150–3154.
13. Stiburkova B, Majewski J, Sebesta I *et al.* Familial juvenile hyperuricemic nephropathy: localization of the gene on chromosome 16p11.2- and evidence for genetic heterogeneity. *Am J Hum Genet* 2000; **66**: 1989–1994.
14. Stacey JM, Turner JJ, Harding B *et al.* Genetic mapping studies of familial juvenile hyperuricemic nephropathy on chromosome 16p11–p13. *J Clin Endocrinol Metab* 2003; **88**: 464–470.
15. Stiburkova B, Majewski J, Hodanova K *et al.* Familial juvenile hyperuricaemic nephropathy (FJHN): linkage analysis in 15 families, physical and transcriptional characterisation of the FJHN critical region on chromosome 16p11.2 and the analysis of seven candidate genes. *Eur J Hum Genet* 2003; **11**: 145–154.
16. Ohno I, Ichida K, Okabe H *et al.* Familial juvenile gouty nephropathy: exclusion of 16p12 from the candidate locus. *Nephron* 2002; **92**: 573–575.
17. Kroiss S, Huck K, Berthold S *et al.* Evidence of further genetic heterogeneity in autosomal dominant medullary cystic kidney disease. *Nephrol Dial Transplant* 2000; **15**: 818–821.
18. Auranen M, Ala-Mello S, Turunen JA *et al.* Further evidence for linkage of autosomal-dominant medullary cystic kidney disease on chromosome 1q21. *Kidney Int* 2001; **60**: 1225–1232.
19. Christodoulou K, Tsingis M, Stavrou C *et al.* Chromosome 1 localization of a gene for autosomal dominant medullary cystic kidney disease. *Hum Mol Genet* 1998; **7**: 905–911.
20. Fuchshuber A, Kroiss S, Karle S *et al.* Refinement of the gene locus for autosomal dominant medullary cystic kidney disease type 1 (MCKD1) and construction of a physical and partial transcriptional map of the region. *Genomics* 2001; **72**: 278–284.
21. Wolf MT, Karle SM, Schwarz S *et al.* Refinement of the critical region for MCKD1 by detection of transcontinental haplotype sharing. *Kidney Int* 2003; **64**: 788–792.
22. Hodanova K, Majewski J, Kublova M *et al.* Mapping of a new candidate locus for uromodulin-associated kidney disease (UAKD) to chromosome 1q41. *Kidney Int* 2005; **68**: 1472–1482.
23. Bingham C, Ellard S, van't Hoff WG *et al.* Atypical familial juvenile hyperuricemic nephropathy associated with a hepatocyte nuclear factor-1beta gene mutation. *Kidney Int* 2003; **63**: 1645–1651.
24. McBride MB, Rigden S, Haycock GB *et al.* Presymptomatic detection of familial juvenile hyperuricaemic nephropathy in children. *Pediatr Nephrol* 1998; **12**: 357–364.
25. Fairbanks L, Cameron J, Venkat-Raman G *et al.* Early treatment with allopurinol in familial juvenile hyperuricaemic nephropathy (FJHN) ameliorates progression of renal disease in long-term studies. *QJM* 2002; **95**: 597–607.
26. Rindler MJ, Naik SS, Li N *et al.* Uromodulin (Tamm–Horsfall glycoprotein/uromucoid) is a phosphatidylinositol-linked membrane protein. *J Biol Chem* 1990; **265**: 20784–20789.
27. van Rooijen JJ, Voskamp AF, Kamerling JP *et al.* Glycosylation sites and site-specific glycosylation in human Tamm–Horsfall glycoprotein. *Glycobiology* 1999; **9**: 21–30.

28. Easton RL, Patankar MS, Clark GF *et al.* Pregnancy-associated changes in the glycosylation of Tamm–Horsfall glycoprotein. Expression of sialyl Lewis(x) sequences on core 2 type O-glycans derived from uromodulin. *J Biol Chem* 2000; **275**: 21928–21938.
29. Moran P, Raab H, Kohr WJ *et al.* Glycophospholipid membrane anchor attachment. Molecular analysis of the cleavage/attachment site. *J Biol Chem* 1991; **266**: 1250–1257.
30. Field MC, Moran P, Li W *et al.* Retention and degradation of proteins containing an uncleaved glycosylphosphatidylinositol signal. *J Biol Chem* 1994; **269**: 10830–10837.
31. Bleyer AJ, Woodard AS, Shihabi Z *et al.* Clinical characterization of a family with a mutation in the uromodulin (Tamm–Horsfall glycoprotein) gene. *Kidney Int* 2003; **64**: 36–42.
32. Short RA, Tuttle KR. Clinical evidence for the influence of uric acid on hypertension, cardiovascular disease, and kidney disease: a statistical modeling perspective. *Semin Nephrol* 2005; **25**: 25–31.
33. Devonald MA, Karet FE. Renal epithelial traffic jams and one-way streets. *J Am Soc Nephrol* 2004; **15**: 1370–1381.
34. Jovine L, Qi H, Williams Z *et al.* The ZP domain is a conserved module for polymerization of extracellular proteins. *Nat Cell Biol* 2002; **4**: 457–461.
35. Rutishauser J, Spiess M. Endoplasmic reticulum storage diseases. *Swiss Med Wkly* 2002; **132**: 211–222.
36. Choi SW, Ryu OH, Choi SJ *et al.* Mutant Tamm–Horsfall glycoprotein accumulation in endoplasmic reticulum induces apoptosis reversed by colchicine and sodium 4-phenylbutyrate. *J Am Soc Nephrol* 2005; **10**: 3006–3014.
37. Bleyer AJ, Hart TC, Shihabi Z *et al.* Mutations in the uromodulin gene decrease urinary excretion of Tamm–Horsfall protein. *Kidney Int* 2004; **66**: 974–977.
38. Devuyst O, Dahan K, Pirson Y. Tamm–Horsfall protein or uromodulin: new ideas about an old molecule. *Nephrol Dial Transplant* 2005; **20**: 1290–1294.
39. Serafini-Cessi F, Malagolini N, Cavallone D. Tamm–Horsfall glycoprotein: biology and clinical relevance. *Am J Kidney Dis* 2003; **42**: 658–676.
40. Gresh L, Fischer E, Reimann A *et al.* A transcriptional network in polycystic kidney disease. *EMBO J* 2004; **23**: 1657–1668.
41. Schmitt R, Kahl T, Mutig K *et al.* Selectively reduced expression of thick ascending limb Tamm–Horsfall protein in hypothyroid kidneys. *Histochem Cell Biol* 2004; **121**: 319–327.
42. Chakraborty J, Below AA, Solaiman D. Tamm–Horsfall protein in patients with kidney damage and diabetes. *Urol Res* 2004; **32**: 79–83.
43. Scolari F, Caridi G, Rampoldi L *et al.* Uromodulin storage diseases: clinical aspects and mechanisms. *Am J Kidney Dis* 2004; **44**: 987–999.
44. Chabardes-Garonne D, Mejean A, Aude JC *et al.* A panoramic view of gene expression in the human kidney. *Proc Natl Acad Sci USA* 2003; **100**: 13710–13715.
45. Bachmann S, Mutig K, Bates J *et al.* Renal effects of Tamm–Horsfall protein (uromodulin) deficiency in mice. *Am J Physiol Renal Physiol* 2005; **288**: F559–F567.
46. Kobayashi K, Fukuoka S. Conditions for solubilization of Tamm–Horsfall protein/uromodulin in human urine and establishment of a sensitive and accurate enzyme-linked immunosorbent assay (ELISA) method. *Arch Biochem Biophys* 2001; **388**: 113–120.
47. Kmoch S, Hartmannova H, Stiburkova B *et al.* Human adenylosuccinate lyase (ADSL), cloning and characterization of full-length cDNA and its isoform, gene structure and molecular basis for ADSL deficiency in six patients. *Hum Mol Genet* 2000; **9**: 1501–1513.
48. Landmann L. Deconvolution improves colocalization analysis of multiple fluorochromes in 3D confocal data sets more than filtering techniques. *J Microsc* 2002; **208**: 134–147.
49. Manders EMM, Verbeek FJ, Aten JA. Measurement of colocalization of objects in dual-color confocal images. *J Microsc* 1993; **169**: 375–382.